THERMOGRAVIMETRIC STUDY OF THE DECOMPOSITION OF PRINTED CIRCUIT BOARDS FROM MOBILE PHONES

Nuria Ortuño, Julia Moltó, Silvia Egea, Rafael Font & Juan A. Conesa

Chemical Engineering Department. University of Alicante. P.O. Box 99, 03080 Alicante (Spain). Phone: + (34) 96 590 38 67 Fax: + (34) 96 590 38 26

Author email address: nuria.ortuno@ua.es

ABSTRACT

Thermal decomposition of printed circuits boards (PCB) is studied, using thermogravimetric analysis to compare the thermal behavior of PCB of mobile phones before and after the removal of the metallic fraction by acid washing. Several dynamic and dynamic+isothermal runs have been carried out at different heating rates (5, 10 and 20 K/min), from room temperature to more than 1100 K. Also runs in the presence and in the absence of oxygen were performed (combustion and pyrolysis runs).

Moreover, TG-MS experiments were performed (both in inert and oxidizing atmosphere) in order to better understand the thermal decomposition of these wastes and identify some compounds emitted during the controlled heating of these materials.

Different reaction models are proposed, one for pyrolysis and one for combustion of the two kinds of wastes studied, which proved to simulate appropriately the experimental results at all the heating rates simultaneously.

KEYWORDS: Pyrolysis, combustion, kinetics, thermogravimetry, printed circuit board.

1. INTRODUCTION

The production of electrical and electronic equipment (EEE) is one of the fastest-growing sectors of the manufacturing industry in the world. At the same time, technological innovation and intense marketing engender a rapid replacement process. Every year, 20–50 million tonnes of waste electrical and electronic equipment (WEEE) are generated worldwide, which could bring serious risks to the human health and the

environment [UNEP, E-waste, the hidden side of IT equipment's manufacturing and use E-waste, the hidden side of IT equipment's manufacturing and use, Environment Alert Bulletin, 2005].

The Electrical and Electronic Equipment Waste Directive [1] promotes the re-use, recycling and recovery of such electrical and electronic waste. The Directive requires the separate collection of electrical and electronic waste as a separate waste stream, which enhances the prospects for economic recycling.

Among these wastes, printed circuit boards are particularly problematic to recycle because of the heterogeneous mix of organic material, metals, and glass fibre [2] and low recycling rates are reported of about 15 % [3]. It has been estimated that PCB comprise approximately 6 wt % of all WEEE, representing over 500,000 tonnes of printed circuit boards generated in the EU27 per year [Das 09 RCR].

The metals present in PCB include large amounts of copper, aluminum and iron, and also precious metals such as gold, silver and palladium, which increase the interest in recycling technologies to recover such metals. In addition, the plastic fraction of the PCB represents an important fraction to meet recycling and recovery targets set out in the WEEE Directive [4]. In the past, the non metallic fractions were treated by combustion, which can lead to the formation of toxic brominated compounds derived from the brominated flame retardants contained in the circuit boards, or sent to landfill, which can lead to toxic compounds leaching to the groundwater [5,6].

Thermogravimetric (TG) analysis is one of the techniques for studying the primary reaction in the decomposition of solids and has been widely used to study the thermal decomposition of PCB waste. The interpretation of the experimental data can provide information on the composition of the sample, order of reaction, number of different processes taking place in the reaction, and the corresponding kinetic constants [7].

Only a few authors proposed kinetic models that simulate the behavior of the thermal degradation of the materials studied. Chien et. al. [8] studied the thermal decomposition of waste printed circuit board using a fixed bed reactor with nitrogen at temperatures of 350 – 800 ºC and thermogravimetric analysis at a heating rate of 5 ºC min^{-1}. Kowalska et al. [9] used TG analysis to study the pyrolysis of a heterogeneous mixture of printed circuit boards (epoxy resin based) obtained from WEEE. Chiang et al. [10] investigated the influence of particle size and process temperature on the pyrolysis of mixed waste

printed circuit boards collected from a recycling plant; pyrolysis was carried out in a laboratory scale quartz tube furnace between 200 and 500 ºC in nitrogen and they also undertook thermogravimetric analysis of the circuit boards to produce pyrolysis kinetic data in relation to sample heating rate. Li et. al. [11] conducted a thermo-analytical and kinetics study on PCBs by TG analysis under various atmospheres and focused on low-temperature scope. Barontini et al. [12] investigated the thermal degradation patterns of the plastic fraction of flame retarded epoxy resin after the removal of metal content, using a thermogravimetric analyser and a laboratory scale pyrolysis reactor; a simplified kinetic analysis was undertaken which considered a single-step first-order autocatalytic kinetic model.

Other authors [5,13-15] studied the pyrolysis of printed circuit boards from different e-wastes, at temperatures ranging from 300 to 800 ºC, and determined the corresponding solid, liquid and gas yields. Finally, some papers addressed the study of the thermal decomposition products of metal free flame retarded epoxy resins [7,16-20].

In a previous study [21], the thermal decomposition of used PCB from mobile phones was studied. The present work uses thermogravimetric analysis to compare the thermal behavior of PCB from mobile phones before and after the removal of the metallic fraction both in the presence and in the absence of oxygen, studies the main gaseous evolved products and proposes a kinetic model for the decomposition of each material.

2. EXPERIMENTAL

2.1. RAW MATERIAL

Two different materials were compared in the present study. On the one hand, waste printed circuit boards from mobile phones were separated and crushed to fine dust (sample named “PCB”) using a vibratory disc mill by Herzog, HSM 100 (Osnabrüch, Germany). On the other hand, in order to remove the metallic fraction, a part of the sample was treated with a dilute aqueous solution of HCl and H_2O_2, followed by washing with deionized water and drying at 110 ºC (sample named “non metallic PCB”).

Table 1 shows the ultimate analysis of both samples, obtained with a CHNS analyzer (FlashEA 1112 Series, ThermoFinnigan), whereas Table 2 shows the semi-quantitative analysis of the remaining elements, performed by X-ray fluorescence with an automatic sequential spectrometer (model TW 1480, PHILIPS MAGIX PRO, Philips Co., Ltd.).

For PCB, copper represents 24.19 wt % (weight percentage), whereas for non metallic samples copper accounts only for 0.50 wt %, confirming the effectiveness of the acid washing treatment. Other metals, such as Ca, Al, Pb, Sn, Ni or Fe, present also lower values in the non metallic PCB sample. Consequently, other elements, as is the case of Si or halogens, show an increase in their concentration in this washed sample.

Tables 1 and 2

2.2. THERMOBALANCE

The experiments of thermogravimetry were performed in a Mettler Toledo thermobalance (model TGA/SDTA851e/LF/1600) with a horizontal furnace and a parallel-guided balance. The position of the sample does not change during the measurement, and flow gas perturbation and thermal buoyancy are minimized. The sample temperature was measured with a sensor directly attached to the sample holder. Good performance of the TG system was checked by carrying out one experiment with Avicel PH-105 microcrystalline cellulose at 5 K min^{-1} in nitrogen and calculating the corresponding kinetic constants of its thermal degradation, which were in good agreement with those obtained in a roundrobin study of Avicel cellulose pyrolysis [22].

Pyrolysis (N_2) and combustion runs, N_2:O_2.= 4:1 (normal conditions) and N_2:O_2 = 9:1 (poor oxygen conditions), were carried out with a flow rate of 100 mL min^{-1}. Dynamic experiments were carried out at three different heating rates (5, 10 and 20 K min^{-1}), from room temperature to a final temperature higher than 1000 K, covering in this way an extensive range of decomposition. Isothermal experiments started with a constant heating rate until the set temperature was reached, and then the final temperature was maintained constant throughout the pyrolysis or combustion process for, at least, 120 minutes; these final temperatures were selected according to the temperatures with the highest weight loss in dynamic runs. The sample mass used was around 5 mg in all cases, and under these conditions, it has been tested that the heat transfer effects are very small.

The TG-MS runs were carried out in the same thermobalance coupled to a Pfeiffer Vacuum mass spectrometer (model Thermostar GSD301T) to monitor the signal of the volatile compounds evolved. Operating conditions for these experiments were as follows: sample mass around 10 mg, heating rate 30 K min^{-1}, ionization 70 eV, SIR mode, atmospheres of He and He:O_2 = 4:1. The response of the different ions was

normalized to that of helium (m/z = 4) and the minimum value was subtracted from each one to relate all the values to zero.

3. RESULTS AND DISCUSSION

3.1. PRINTED CIRCUIT BOARDS ("PCB" SAMPLE)

3.1.1. THERMOGRAVIMETRIC STUDY

In order to study thermal decomposition of printed circuit boards ("PCB" sample), several pyrolysis and combustion runs have been carried out in dynamic mode (constant heating rate) or isothermal mode (constant heating rate until the set temperature is reached and then constant temperature). Figure 1 shows the results in the presence of nitrogen (pyrolysis runs). Figures 2 and 3 are the corresponding to 20 and 10 % of oxygen respectively. In the figures, the weight fraction (on the left Y axis) represents the residual mass fraction of the solid, i.e., the sum of the residue formed and the non-reacted solid.

Figure 1A shows the TG plots for pyrolysis at three heating rates: 5, 10 and 20 K min^{-1}. For the 20 K min^{-1} run, Figure 1A also shows the ΔT corresponding to the differential thermal analysis (DTA). ΔT value is shown on the right Y-axis, and it is plotted in a convenient scale, from –10 K for a strong endothermic process to +10 K corresponding to a strong exothermic process. It can be concluded that there is neither a great heat release nor consumption in these runs.

Figure 1B shows TG and derivative thermogravimetric analysis (DTG) curves for the pyrolysis run at 20 K min^{-1}. It can be observed that there is an initial large peak (with the maximum decomposition rate at 630 K) followed by a small band or wide peak (from 680 to 800 K), which means that at least two fractions must be considered in the decomposition, with a final residue of around 76 % of initial sample weight.

Three isothermal runs were carried out in pyrolytic conditions (Figure 1C). These experiments started with constant heating rate until the desired temperature was reached, and then the final temperature was maintained throughout the pyrolysis process.

Figure 1

Figure 2A shows the experimental TG plots of combustion runs (N_2:O_2 = 4:1) at three heating rates (5, 10, 20 K min^{-1}). The ΔT corresponding to the differential thermal

analysis (DTA) is also plotted for the run at 20 K min^{-1}. It can be observed that a small exothermic band due to oxidative pyrolysis appears, and later a significant exothermic process takes place in the last part of the decomposition due to strong oxidation.

Figure 2B shows TG and DTG runs for the combustion at 10 K min^{-1}. From the DTG curve, it can be observed that there is an initial large peak, with the maximum decomposition rate at 630 K that coincides with the first process observed in pyrolysis. This is followed by a second peak at around 665 K followed by a decreasing peak at 770 K that stands for the oxidation of the metallic fraction. Lastly, a third increasing peak is observed with maximum decomposition rate at 800 K, leading to a solid residue yield of 85 wt %. The decomposition of the complete printed circuit board takes place in three different processes, suggesting that at least three fractions must be considered in the decomposition, apart from the oxidizing step.

The results of isothermal runs in a 4:1 N_2:O_2 atmosphere and at different heating rates are shown in Figure 2C.

Figure 2

Figure 3A and 3B show the experimental results for dynamic and isothermal runs in a 9:1 N_2:O_2 atmosphere, with similar behavior to that observed with 4:1 N_2:O_2 atmosphere.

Figure 3

The main decomposition range of the residues studied in this paper is 570 – 750 K and coincides with the previously reported by Moltó et. al. [21].

Comparing the results with other studies, the thermogravimetric analysis conducted by Kowalska et al. [9] on the pyrolysis of three types of printed circuit boards indicated a solid residue yield of ~74 wt % and two maxima of DTG at 593 and 629 K were observed, but these two peaks were caused not only by dissimilar resins, being part of both samples (epoxy resin and polyester resin) but also by different flame retardants used as components. The results showed that the decomposition took place mainly in the range 573 – 673 K, and at temperatures above 673 K, there was a slow decomposition.

Hall and Williams [5] presented a TG pyrolysis run of mixed waste electrical and electronic equipment. In this case the decomposition took place in the range 673 – 823 K, a little wider than that of the residues considered in the present paper.

According to Li et. al. [11], PCB degradation in air is clearly divided into three steps: in step one (< 570 K), mass loss was restricted to a minimum level; in step two (570 - 673 K), the flame retardant decomposed and the gas or liquid products were released and in step three (> 673 K), the TG curve returned to a smooth decrease, because a large amount of the organic material was decomposed into gas and liquid products. These stages coincide with the ones observed in the present study, although the weight gain peak is not observed because these authors only carried out experiments up to 673 K, delimiting the beginning of the metallic fraction oxidation.

3.1.2. STUDY OF THE EMISSIONS BY TG-MS

Different TG-MS run were carried out analyzing the evolution of the most relevant ions in two atmospheres (He and He:O_2 = 4:1). All the runs were performed from room temperature to more than 1000 K, at a heating rate of 30 K min^{-1}. The results were carefully evaluated to determine the majority evolving compounds (considering the relative abundances of the different fragments of each compound), since different ionic species with the same m/z ratio can be easily mistaken. The evolution of some masses corresponding to brominated compounds was followed but any of them was detected, because the sensitivity of the mass spectrometer employed decreased rapidly for ions with high m/z values.

Figure 4A shows the variation of ions 18, 28 and 44 of a pyrolysis run, corresponding to water, CO and CO_2, which are the main gaseous products. Figure 4B shows the response of ions with m/z equal to 16 (methane), 27 (ethylene), 41 (propylene) and 94 (phenol) in the same atmosphere. At a heating rate of 30 K min^{-1}, those compounds are mostly emitted around 610 K, although methane is also emitted at around 800 K, thus confirming that there are at least two fractions with different reactivity under pyrolytic conditions.

For the runs carried out under oxidizing atmosphere (He:O_2 = 4:1), Figure 4C shows that the main gaseous products are the same as in pyrolysis: water (m/z 18), CO (m/z 28) and CO_2 (m/z 44), but in that case three stages are observed during the evolution of CO and CO_2 (at around 620, 690 and 800 K), whereas water is emitted in a wide range

of temperatures (500 – 800 K). Those peaks indicate that in addition to the two fractions deduced in the pyrolysis, there are two more fractions, corresponding to an intermediate oxidation or "oxidative pyrolysis" (second peak) and the oxidation of the metallic fraction, that leads to an increase in weight. Apart from that, only ethylene is detected (Figure 4D) at around 600 K, indicating that compounds such as methane, propylene and phenol have been oxidized.

Figure 4

With a comparison on literature sources subjected to N_2 or air atmosphere, while the products released during the first phase were mainly H_2O and CO_2, the flame retardants and other plastic additives were decomposed or volatilized, releasing small-molecule products within the second phase, including HBr, H_2O, CO_2 and molecular hydrocarbons (methane, ethane, and butane). Gases and liquid substances were released from resin decomposition during the third phase; indicating that complete pyrolysis and carbonization occurred [11].

3.1.3. KINETIC MODEL

Different kinetic models were applied in order to simultaneously fit all TG curves under dynamic and isothermal conditions. The range of temperatures used for the kinetic calculation has been the complete range of decomposition, i.e., 350-1000 K. Above this temperature, there are no other processes.

In a previous work by Molto et al. [21] a complex kinetic model was presented for the thermal decomposition of PCB from mobile phones, in similar conditions to the ones applied in the present study. The model presented was not able to reproduce the increase of the weigth due to the oxidation of the metallic fraction of the sample. In the present work the model has been significantly simplified, and, as will be shown later, it will be able to explain the increase in the weight.

The kinetic model proposed for the pyrolysis of PCB could be interpreted considering the material formed by three independent parts, each one following an independent reaction, as follows:

$$w_{s_{10}}\,\mathrm{Solid}_1 \xrightarrow{1} (w_{s_{10}} - v_{1\infty})\,\mathrm{Residue}_1 + v_{1\infty}\,\mathrm{Volatiles}_1 \quad (1)$$

$$w_{s_{20}}\,\mathrm{Solid}_2 \xrightarrow{2} (w_{s_{20}} - v_{2\infty})\,\mathrm{Residue}_2 + v_{2\infty}\,\mathrm{Volatiles}_2 \quad (2)$$

247 $$w_{s_{30}}\,\mathrm{Solid}_3 \xrightarrow{3} (w_{s_{30}} - v_{3\infty})\,\mathrm{Residue}_2 + v_{3\infty}\,\mathrm{Volatiles}_3 \quad (3)$$

248 Solid_i refers to the different fractions of the original material (i = 1 to 3), $\mathrm{Volatiles}_i$ are
249 the gases and volatiles evolved in the corresponding reactions, and $\mathrm{Residue}_i$ is the
250 possible residue formed in the decomposition of each Solid_i. Lower case letters
251 represent the yield coefficients representative of each reaction and, consequently, it is
252 considered that they do not change with time or with the extension of the reaction. Each
253 fraction has a yield coefficient that represents the maximum mass fraction obtainable by
254 each reaction. In this way, $v_{i\infty}$ is the yield coefficient for the $\mathrm{Volatiles}_i$ that coincides
255 with the maximum mass fraction of volatiles that can be evolved at infinite time.

256 The conversion degree for each reaction is defined as the ratio between the mass
257 fraction of solid reacted at any time ($w_{si0} - w_{si}$) and the corresponding initial fraction of
258 this component w_{si0}, or the ratio between the mass fraction of volatiles obtained at any
259 time during which the reaction is taking place V_i and the corresponding yield coefficient
260 $v_{i\infty}$, so:

261 $$\alpha_i = \frac{w_{s_{i0}} - w_{s_i}}{w_{s_{i0}}} = \frac{V_i}{v_{i\infty}} \qquad \text{for i = 1 to 3} \quad (4)$$

262 where w_{si0} is the weight fraction of each Solid_i in the original material, and
263 consequently:

264 $$\sum_{i=0}^{3} w_{s_{i0}} = 1 \quad (5)$$

265 From the mass balance between products and reactants and the conversion degrees, the
266 kinetic equations for the pyrolysis runs can be expressed as follow:

267 $$-\frac{d\left(\frac{w_{s_i}}{w_{s_{i0}}}\right)}{dt} = \frac{d\left(\frac{V_i}{v_{i\infty}}\right)}{dt} = \frac{d\alpha_i}{dt} = k_i\left(\frac{w_{si}}{w_{s_{i0}}}\right)^{n_i} = k_i(1-\alpha_i)^{n_i} = k_i\left[1-\frac{V_i}{v_{i\infty}}\right]^{n_i} \quad (6)$$

268 with the kinetic constants following the Arrhenius equation:

269 $$k_i = k_{i0}\exp\left(-\frac{E_i}{RT}\right) \qquad \text{for i = 1 to 3} \quad (7)$$

270 By integration of these equations, it is possible to calculate α_i at each time if the
271 temperature program T(t) is known. The relationship between α_i values and the weight

fraction measured in the thermobalance (w) is related with the total volatile fraction obtained (V) by:

$$w = 1 - V = 1 - F_V\left(v_{1\infty}\alpha_1 + v_{2\infty}\alpha_2 + v_{3\infty}\alpha_3\right) \quad (8)$$

In the previous equation, a correcting factor F_V has been introduced due to the fact that the samples can have a slight but significant different content of inert material, due to the heterogeneity of the samples studied. In all the cases the values F_V considered are between 0.99 and 1.05.

For combustion reactions, the proposed scheme considers four initial solid fractions. One of them accounts for the oxidation of metallic fractions, where the sample increases its weight due to the formation of oxides and the other three fractions are equivalent to those shown in pyrolytic conditions. The scheme proposed is the following one:

- Organic matter decomposition: three pyrolytic reactions:

$$w_{s_{10}}\,\mathrm{Solid}_1 \xrightarrow{1} (w_{s_{10}} - v_{1\infty})\mathrm{Residue}_1 + v_{1\infty}\mathrm{Volatiles}_1 \quad (9)$$

$$w_{s_{20}}\,\mathrm{Solid}_2 \xrightarrow{2} (w_{s_{20}} - v_{2\infty})\mathrm{Residue}_2 + v_{2\infty}\mathrm{Volatiles}_2 \quad (10)$$

$$w_{s_{30}}\,\mathrm{Solid}_3 \xrightarrow{3} (w_{s_{30}} - v_{3\infty})\mathrm{Residue}_3 + v_{3\infty}\mathrm{Volatiles}_3 \quad (11)$$

- Metal oxidation: one fraction is considered where there is an increase of weight.

$$w_{s_{40}}\,\mathrm{Solid}_4 + v_{4\infty}\mathrm{O}_2 \xrightarrow{4} (w_{s_{40}} + v_{4\infty})\mathrm{Residue}_4 \quad (12)$$

The kinetic equations, considering conversion degrees are the following:

$$\frac{d\alpha_i}{dt} = k_i\left(1-\alpha_i\right)^{n_i} \qquad \text{for i = 1 to 4} \quad (13)$$

The dependence of oxygen has been considered with the following expressions:

$$k_{i0}^{*} = k_{i0}\left[\frac{p_{O2}}{0.20}\right]^{b} \quad (14)$$

where the pre-exponential factor k_{i0} is directly proportional to the oxygen pressure, and p_{O2} is the partial pressure of oxygen in atm. Logically, k_{i0}^{*} equals k_{i0} working with N_2:O_2 = 4:1 atmosphere (p_{O2} equals 0.20 atm). The values of coefficient b have been obtained for each reaction.

The total weight fraction (w) and the volatile weight fraction (V) are related with the conversion degrees by:

$$w = 1 - V = 1 - F_P\left(v_{1\infty}\alpha_1 + v_{2\infty}\alpha_2 + v_{3\infty}\alpha_3\right) + F_M\left(v_{4\infty}\alpha_4\right) \quad (15)$$

where $v_{i\infty}$ represent the maximum values in accordance with the scheme of reactions proposed, and F_P and F_M are, respectively, weight factors corresponding to the polymeric fraction that can decompose and to the metal fraction that can be oxidized. In this case, this weight factors obtained also by optimization vary between 0.90 and 1.10. It must be emphasized that these factors are included considering that each sample can contain different quantities of fractions that can be decomposed or oxidized. In duplicated runs, it has been tested that the volatile mass evolved at infinite time in TG runs can be slightly different from one sample to another.

The correlation parameters were obtained by integration of the differential equations presented in the kinetic model, with the Euler method, but considering and testing that the intervals of time were small enough, so the errors introduced are negligible. The optimization was done by using Solver function in an Excel spreadsheet, minimizing the differences between experimental and calculated weight loss values and their derivatives. The objective function to minimize was the sum of the square differences between experimental and calculated total volatile V:

$$OF = \sum_{m=1}^{M}\sum_{j=1}^{N}\left(V_{m,j}^{exp} - V_{m,j}^{cal}\right)^2 \quad (16)$$

where M is the number of runs and N is the number of points in each run.

The model validity was tested calculating the variation coefficient (VC):

$$VC = \frac{\sqrt{\frac{OF}{N_{total} - P}}}{\overline{V_{exp}}} \cdot 100 \quad (17)$$

where N_{total} and P are the number of data and parameters fitted, respectively, and $\overline{V_{exp}}$ is the average of the experimental values of weight fraction corresponding to the volatiles evolved.

The kinetic parameters obtained are shown in Table 3. The calculated curves are shown in Figures 1, 2 and 3, where the experimental data are also presented, overlapping the

experimental curves in most cases. The mean variation coefficient for the correlation of all experimental data (dynamic and isothermal runs at different heating rates) by using the same kinetic constants, and considering the weight fraction of volatiles evolved, is 1.4 % for pyrolysis and 5.4 % for combustion, which are relatively small values.

Table 3

Figure 5 shows the contribution of each reaction in the decomposition process. In Figure 5A the mass fractions of the residues in the three pyrolytic processes are shown; it can be observed that there are two main fractions (1 and 2). In Figure 5B, corresponding to the combustion process, the residues corresponding to all reactions can be observed, showing that all the reactions implied are important in the satisfactory correlation of the data.

Figure 5

To obtain a single set of parameters for the pyrolysis and for the combustion kinetic models for printed circuit boards, all the runs were correlated simultanously in order to obtain only one set of parameters valid for any condition.

3.2. METAL FREE PRINTED CIRCUIT BOARDS ("NON METALLIC PCB" SAMPLE)

3.2.1. THERMOGRAVIMETRIC STUDY

In order to compare the thermal behavior of printed circuit boards before and after metal removal, the same set of pyrolysis and combustion runs were carried out with the "non metallic PCB" sample. In summary, nine dynamic experiments were carried out by combining three different atmospheres (N_2, N_2:O_2 = 9:1 and N_2:O_2 = 4:1) and three heating rates (5, 10 and 20 K min^{-1}) from room temperature to more than 1100 K, and other nine dynamic + isothermal runs were performed (same final temperatures as for the PCB sample). Figures 6 to 8 show the experimental results.

Figure 6A shows the TG plots for pyrolysis at three heating rates: 5, 10 and 20 K min^{-1}, as well as the DTA increment of temperature for the 20 K min^{-1} run that shows that no great heat release nor consumptions occurs in these runs. Figure 6B shows TG and DTG curves for the pyrolysis run at 20 K min^{-1}. As for the PCB sample, an initial large peak (with a maximum in DTG at 615 K) followed by a small band is observed (also from 680 to 800 K), that leads to a solid yield of 50 wt %; this suggests to consider at least

two fractions in the decomposition of the non metallic PCB sample. Figure 6C shows the isothermal runs carried out in pyrolytic conditions at three different final temperatures and initial heating rates.

Figure 6

Figure 7A shows the experimental TG plots of combustion runs (N_2:O_2 = 4:1) at 5, 10 and 20 K min^{-1} and the ΔT curve at 20 K min^{-1}. A wide exothermic peak is observed in DTA analysis, formed by three consecutive smaller peaks that correspond to a strong oxidation of the sample. Figure 7B shows TG and DTG curves for the combustion at 20 K min^{-1}. In oxygen presence, an initial large peak is observed at around 610 K in the DTG run; as for the PCB sample, this peak coincides with the first process observed in pyrolysis (Figure 6B). A little peak appears at 735 K and a third bigger DTG peak is observed at 800 K, producing a final solid residue of about 39 wt %. In this way, these observations confirm that the decomposition of the metal free circuit boards takes place in three different processes. The isothermal runs at different heating rates in 4:1 N_2:O_2 atmosphere are shown in Figure 7C.

Figure 7

Figure 8 shows the experimental results for dynamic and isothermal runs in a 9:1 N_2:O_2 atmosphere, with similar behavior to that observed with 4:1 N_2:O_2 atmosphere.

Figure 8

The main decomposition temperature range observed for non metallic PCB in this work is 570 – 750 K (as it happened for PCB sample). This range is a little wider, but still in good agreement with the data reported in previous studies, which suggest that the thermal degradation process of the organic components of electronic scrap at low heating rates takes place at temperatures between 550 and 650 K [23-25].

For non metallic PCB, the first weight loss process starts at similar temperatures in inert and oxidizing environments, indicating that this stage does not depend on the presence of oxygen; however, a higher residue results from this decomposition step in the presence of oxygen. A higher thermal stability in air at temperatures between 523 and 673 K was reported in the literature for several materials (e.g., diisocyanates, polyurethanes, etc.), and was attributed to the occurrence of cross-linking and condensation radical reactions during the thermal decomposition [12]. The second stage occurs over a longer temperature range compared to the one in air due to decomposition

and release of various fragments over different temperature ranges [26]. On the other hand, in air, some fragments begin to be oxidized whilst the resin is decomposing [18].

Biswas et. al. [18] also reported three stages in the degradation of pure epoxy uncured resin in air at 10 K min^{-1}: a first stage due to water loss through curing and dehydration (up to 538 K) with 10 % mass loss, a second stage due to the decomposition to a char (623 – 733 K) with 30 % mass loss and a third stage corresponding to char oxidation (713 – 893 K) with 57 % mass loss leaving 2.5 % char residue at the end. In nitrogen atmosphere, only two stages were reported: a first stage (up to 538 K) with 8 % mass loss and a second stage in the temperature range (632 – 795 K) with 62% mass loss leaving 29.9 % char residue at 1173 K

3.1.2. STUDY OF THE EMISSIONS BY TG-MS

Experimental results of different TG-MS runs for the metal free sample (non metallic PCB) are shown in Figure 9. Figure 9A shows the evolution of water (m/z 18), carbon dioxide (m/z 44) and carbon monoxide (m/z 28) at around 600 K in pyrolysis. In Figure 9B, two peaks can be observed for the evolution of methane (m/z 16) and ethylene (m/z 27) at 600 and 800 K, whereas propylene (m/z 41) and phenol (m/z 94) are mostly emitted at the low temperature peak.

Figure 9C and 9D shows the results for the runs carried out under oxidizing atmosphere (He:O_2 4:1). Here, the main gaseous products are also water, CO and CO_2, but in oxygen presence evolution of water (m/z 18) occurs in a wider temperature range, between 470 and 900 K, with the highest emission rate at around 590 K, whereas CO and CO_2, which are emitted along a similar temperature range, present a maximum at around 780 K. Ethylene is detected (Figure 9D) at around 600 K, indicating that compounds such as methane, propylene and phenol has been oxidized, as happened with the PCB sample.

Figure 9

Barontini et al. [12,17] used TGA-FTIR and a small batch reactor to investigate the pyrolysis of the plastic fraction of flame retarded epoxy resin, after the removal of metals, and reported that the most prominent gas was HBr followed by CO_2 and CO; only small amounts of CH_4 were reported. The evolution of CO and CO_2 was mainly detected during the second step of the thermal degradation of electronic boards in air (623 - 823 K). This confirms that this second weight loss step is mainly due to the

oxidation of the residual char formed at lower temperatures (during the main thermal degradation process identified by the first weight loss step).

3.2.3. KINETIC MODEL

In this section, the same methodology and nomenclature is observed as for the PCB sample (see Section 3.1.3).

Similarly to the one proposed for printed circuit boards, three fractions have been considered in the pyrolysis kinetic model (see Eq. 1, 2 and 3).

For combustion, the scheme selected considers the same initial solid fractions and the same reactions as the pyrolysis model. In this case, unlike the model for PCB samples, no reaction considers the oxidation of metallic fractions, since this fraction has been removed by acid washing. Furthermore, the TG curve in oxygen atmosphere does not indicate an increase of the weight due to the formation of metal oxides, as was the case for non washed PCB sample.

The total weight fraction (w) and the volatile weight fraction (V) are related with the conversion degrees by Eq. (8), where the factor F_V ranges between 0.90 and 1.10 for all runs.

The correlation parameters were obtained in the same way as for PCB and the results are shown in Table 4. The calculated curves are also shown in Figures 6 to 8, together with the experimental data. The mean variation coefficient for the correlation of experimental data, considering the weight fraction of volatiles evolved is 1.7 % for the pyrolytic model and 4.6 % for the combustion one, which indicate that correlations are satisfactory.

Table 4

Figure 10 shows the contribution of each reaction in the decomposition process. In Figure 10A the evolution of the residue mass fractions in the pyrolytic processes are shown and, as in the PCB, reactions 1 and 2 are the most relevant. In Figure 10B, the residues corresponding to each fraction in the combustion process are shown, where all the reactions implied are important in the satisfactory correlation of the data.

Figure 10

Comparing results for PCB and non-metallic PCB samples, in pyrolysis runs, where only the organic polymer decomposes, the final residue is approximately the same for

all the runs, although the residue from the non metallic sample is much lower (50 versus 76 wt %).

In the presence of oxygen, the PCB sample presents an oxidation of the metallic compounds and this probably generates a different residue at infinite time. As proposed by Moltó et. al. [21], the presence of metals and other compounds catalyzes the decomposition of the organic matter. Also, an increase of weight is observed due to the formation of metallic oxides that lately decompose. Support of this idea is found in the behavior of the non metallic PCB sample, where no weight gain is observed.

4. CONCLUSIONS

The thermal behavior of printed circuit boards, before and after metal removal, has been studied through thermogravimetric analysis under several different operating conditions and the evolution of the main gaseous compounds has been analyzed by TG-MS.

Different kinetic models for the pyrolysis and combustion of these materials are proposed, for which one set of parameters can explain many experiments under different operating conditions. An acceptable correlation can be obtained for dynamic runs at different heating rates and isothermal runs at distinct temperature operation.

ACKNOWLEDGMENTS

Support for this work was provided by the Generalitat Valenciana (Spain), research project Prometeo/2009/043/FEDER, and by the Spanish MCT, research project CTQ2008-05520.

REFERENCES

[1] E. Comission, in Official Journal of the European Comission, Brussels, 2003.

[2] P. Williams, Valorization of Printed Circuit Boards from Waste Electrical and Electronic Equipment by Pyrolysis, Waste and Biomass Valorization 1 (2010) 107-120.

[3] M. Goosey, R. Kellner, in, Intellect and the Department of Trade and Industry, London, 2002.

[4] M. Schlummer, L. Gruber, A. Mäurer, G. Wolz, R. van Eldik, Characterisation of polymer fractions from waste electrical and electronic equipment (WEEE) and implications for waste management, Chemosphere 67 (2007) 1866-1876.

[5] W.J. Hall, P.T. Williams, Separation and recovery of materials from scrap printed circuit boards, Resources, Conservation and Recycling 51 (2007) 691-709.

[6] H. Li, L. Yu, G. Sheng, J. Fu, P.a. Peng, Severe PCDD/F and PBDD/F Pollution in Air around an Electronic Waste Dismantling Area in China, Environ. Sci. Technol. 41 (2007) 5641-5646.

[7] C. Quan, A. Li, N. Gao, Thermogravimetric analysis and kinetic study on large particles of printed circuit board wastes, Waste Management 29 (2009) 2353-2360.

[8] Y.-C. Chien, H. Paul Wang, K.-S. Lin, Y.J. Huang, Y.W. Yang, Fate of bromine in pyrolysis of printed circuit board wastes, Chemosphere 40 (2000) 383-387.

[9] E. Kowalska, J. Radomska, P. Konarski, R. Diduszko, J. Oszczudłowski, T. Opalińska, M. Więch, Z. Duszyc, Thermogravimetric investigation of wastes from electrical and electronic equipment (WEEE), J. Therm. Anal. Calorim. 86 (2006) 137-140.

[10] H.-L. Chiang, K.-H. Lin, M.-H. Lai, T.-C. Chen, S.-Y. Ma, Pyrolysis characteristics of integrated circuit boards at various particle sizes and temperatures, J. Hazard. Mater. 149 (2007) 151-159.

[11] J. Li, H. Duan, K. Yu, L. Liu, S. Wang, Characteristic of low-temperature pyrolysis of printed circuit boards subjected to various atmosphere, Resources, Conservation and Recycling 54 (2010) 810-815.

[12] F. Barontini, K. Marsanich, L. Petarca, V. Cozzani, Thermal Degradation and Decomposition Products of Electronic Boards Containing BFRs, Ind. Eng. Chem. Res. 44 (2005) 4186-4199.

[13] I. de Marco, B.M. Caballero, M.J. Chomón, M.F. Laresgoiti, A. Torres, G. Fernández, S. Arnaiz, Pyrolysis of electrical and electronic wastes, J. Anal. Appl. Pyrolysis 82 (2008) 179-183.

[14] G. Jie, L. Ying-Shun, L. Mai-Xi, Product characterization of waste printed circuit board by pyrolysis, J. Anal. Appl. Pyrolysis 83 (2008) 185-189.

[15] C. Vasile, M.A. Brebu, M. Totolin, J. Yanik, T. Karayildirim, H. Darie, Feedstock Recycling from the Printed Circuit Boards of Used Computers, Energy Fuels 22 (2008) 1658-1665.

[16] M.P. Luda, A.I. Balabanovich, G. Camino, Thermal decomposition of fire retardant brominated epoxy resins, J. Anal. Appl. Pyrolysis 65 (2002) 25-40.

[17] F. Barontini, V. Cozzani, Formation of hydrogen bromide and organobrominated compounds in the thermal degradation of electronic boards, J. Anal. Appl. Pyrolysis 77 (2006) 41-55.

[18] B. Biswas, B.K. Kandola, A.R. Horrocks, D. Price, A quantitative study of carbon monoxide and carbon dioxide evolution during thermal degradation of flame retarded epoxy resins, Polym. Degrad. Stab. 92 (2007) 765-776.
[19] M.P. Luda, A.I. Balabanovich, M. Zanetti, D. Guaratto, Thermal decomposition of fire retardant brominated epoxy resins cured with different nitrogen containing hardeners, Polym. Degrad. Stab. 92 (2007) 1088-1100.
[20] G. Grause, M. Furusawa, A. Okuwaki, T. Yoshioka, Pyrolysis of tetrabromobisphenol-A containing paper laminated printed circuit boards, Chemosphere 71 (2008) 872-878.
[21] J. Moltó, R. Font, A. Gálvez, J.A. Conesa, Pyrolysis and combustion of electronic wastes, J. Anal. Appl. Pyrolysis 84 (2009) 68-78.
[22] M. Grønli, M.J. Antal, G. Varhegyi, A Round-Robin Study of Cellulose Pyrolysis Kinetics by Thermogravimetry, Ind. Eng. Chem. Res. 38 (1999) 2238-2244.
[23] M. Webb, P.M. Last, C. Breen, Synergic chemical analysis – the coupling of TG with FTIR, MS and GC-MS: 1. The determination of the gases released during the thermal oxidation of a printed circuit board, Thermochim. Acta 326 (1999) 151-158.
[24] M. Blazsó, Z. Czégény, C. Csoma, Pyrolysis and debromination of flame retarded polymers of electronic scrap studied by analytical pyrolysis, J. Anal. Appl. Pyrolysis 64 (2002) 249-261.
[25] C. Mazzocchia, A. Kaddouri, G. Modica, R. Nannicini, G. Audisio, C. Barbieri, F. Bertini, Hardware components wastes pyrolysis: energy recovery and liquid fraction valorisation, J. Anal. Appl. Pyrolysis 70 (2003) 263-276.
[26] B.K. Kandola, A.R. Horrocks, P. Myler, D. Blair, in *Fire and Polymers*, American Chemical Society, 2001, p. 344-360.

546 Table 1. Ultimate analysis of the materials used.

547

wt %	PCB	non metallic-PCB
C	20.4	36.4
H	1.9	3.4
N	0.7	1.4
S	nd	nd
O and ash (by difference)	77.0	58.7

nd: not detected

548

549

550 Table 2. Fluorescence analysis of the material used.

551

wt %	PCB	non metallic-PCB
O	24.49	21.73
Cu	24.19	0.50
Si	10.48	15.27
Br	5.67	12.16
Ca	4.52	3.78
Al	3.27	1.53
Pb	0.89	0.03
Sn	1.42	0.47
Ni	0.29	0.06
Ba	0.16	0.69
P	0.40	0.45
Fe	0.16	0.12
Ti	0.15	0.21
S	0.19	0.16
Cl	0.13	1.04
Ag	0.10	0.08
I	0.10	n.d.
Au	0.06	0.14
Zn	0.07	0.01
Mg	0.19	0.13
Sr	0.05	0.07
K	0.03	0.03
Cr	0.02	n.d.
Zr	0.03	0.04
Nb	0.01	n.d.
Nd	n.d.	0.05

nd: not detected

552

553

554 Table 3. Kinetic parameters obtained for the pyrolysis and combustion models of
555 printed circuit boards (PCB sample).

556

Reaction	$v_{i\infty}$	k_{io} (s^{-1})	E_i (kJ mol^{-1})	n_i	b (for O_2)
Pyrolysis					
1	0.120	$1.242 \cdot 10^{11}$	154.4	0.87	-
2	0.107	$2.600 \cdot 10^{23}$	300.2	8.00	-
3	0.124	0.2279	67.1	6.00	-
VC (%)	1.4				
Combustion					
1	0.080	$1.243 \cdot 10^{11}$	165.0	1.40	0.66
2	0.085	$2.600 \cdot 10^{23}$	272.3	4.76	0.66
3	0.110	$1.639 \cdot 10^{4}$	96.7	0.69	0.66
4	0.102	$4.401 \cdot 10^{4}$	98.2	0.41	0.72
VC (%)	5.4				

557

558

559 Table 4. Kinetic parameters obtained for the pyrolysis and combustion models of the
560 non-metallic fraction of printed circuit boards (non-metallic PCB sample).

561

Reaction	$v_{i\infty}$	k_{io} (s^{-1})	E_i (kJ mol^{-1})	n_i	b (for O_2)
Pyrolysis					
1	0.285	$7.418 \cdot 10^{12}$	170.5	1.15	-
2	0.208	$1.630 \cdot 10^{21}$	280.4	4.89	-
3	0.112	44.11	88.6	8.00	-
VC (%)	1.7				
Combustion					
1	0.250	$7.418 \cdot 10^{12}$	170.5	1.15	0.05
2	0.040	$1.630 \cdot 10^{21}$	280.4	4.89	0.05
3	0.330	$7.195 \cdot 10^{7}$	146.6	1.72	0.05
VC (%)	4.6				

562

563

564 Figure 1. Different pyrolysis runs of printed circuit boards: (A) Dynamic experimental
565 runs at three heating rates (the calculated curves overlap the experimental ones) and
566 DTA curve for the run at 20 K min^{-1}. (B) TG and DTG curves (experimental and
567 calculated) at 20 K min^{-1}. (C) Isothermal TG curves (experimental and calculated) at
568 different heating rates.

569

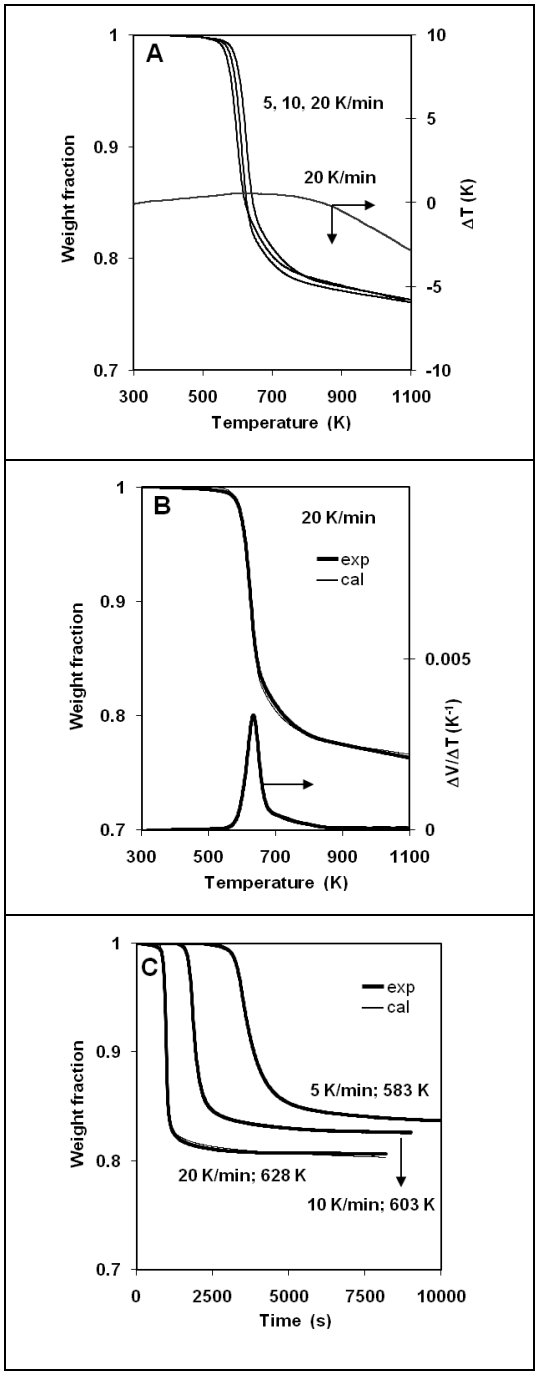

570

571

572 Figure 2. Different combustion (N_2:O_2 = 4:1) runs of printed circuit boards
573 (experimental and calculated curves): (A) Dynamic TG curves at 5, 10 and 20 K min^{-1}
574 and DTA curve for the run at 20 K min^{-1}. (B) TG and DTG curves at 10 K min^{-1}. (C)
575 TG isothermal curves at different heating rates.

576 REVISAR FIGURAS DESDE AQUÍ

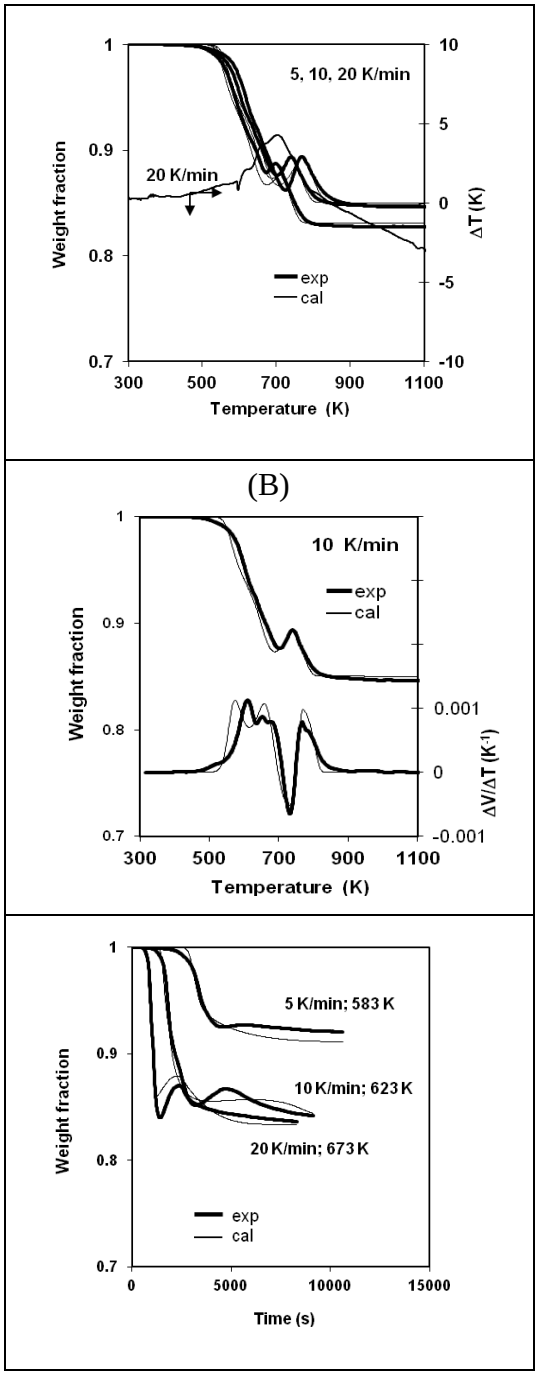

577

578

579 Figure 3. Different combustion (N_2:O_2 = 9:1) runs of printed circuit boards at 5, 10 and
580 20 K min^{-1} (experimental and calculated curves): (A) Dynamic TG runs. (B) Isothermal
581 TG runs.

582

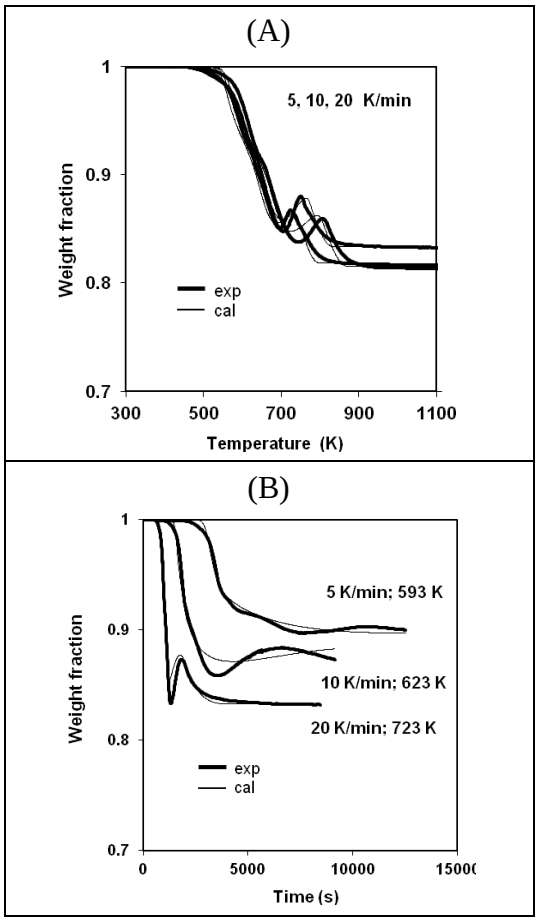

583

584

585 Figure 4. TG-MS of printed circuit boards at a heating rate of 30 K min^{-1}: (A) Intensity
586 of ions m/z 18 (water), 28 (CO) and 44 (CO_2) in pyrolysis (He). (B) Intensity of ions
587 m/z 16 (methane), 27 (ethylene), 41 (propylene) and 94 (phenol) in pyrolysis (He). (C)
588 and (D) Intensity of the same ions as (A) and (B) in combustion (He:O_2 4:1).

589

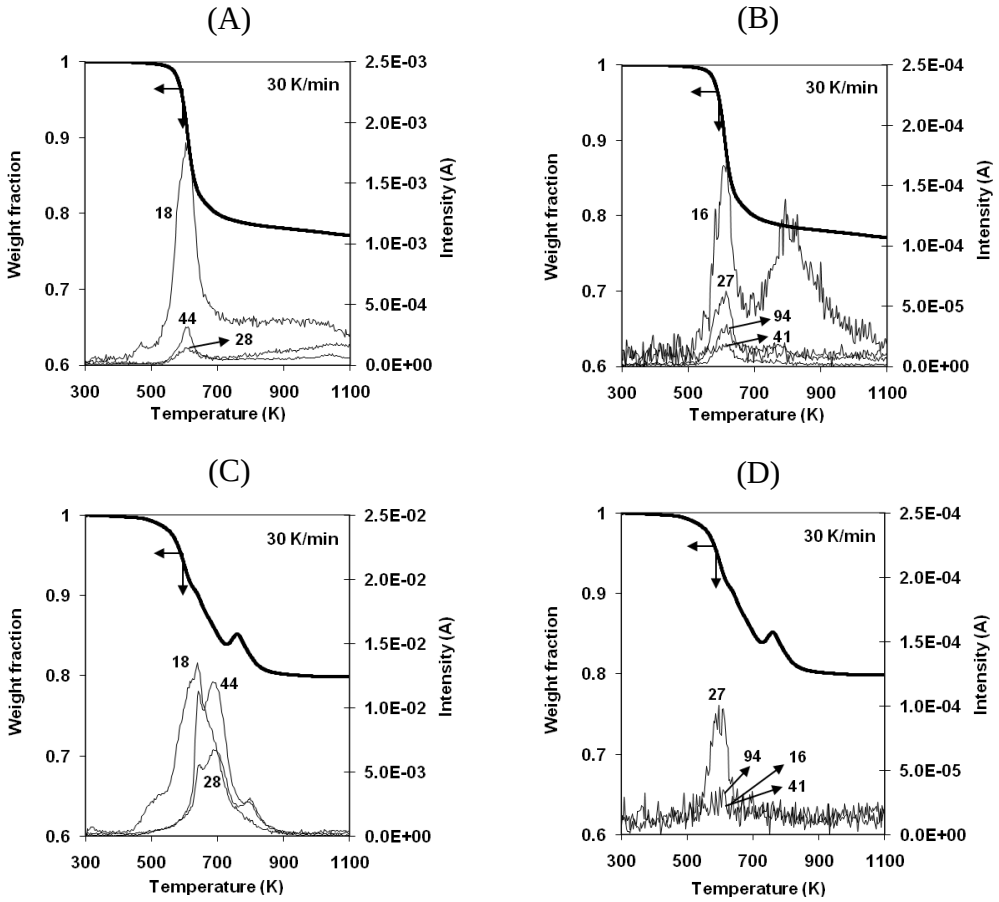

590

591

Figure 5. Evolution of the weight mass and the weight fraction of residues for each reaction, PCB sample: (A) Pyrolysis TG run. (B) Combustion TG run (N_2:O_2 = 4:1 atmosphere).

CAMBIAR PARA QUE SE VEA COMO SUBE LA FRACCIÓN 4

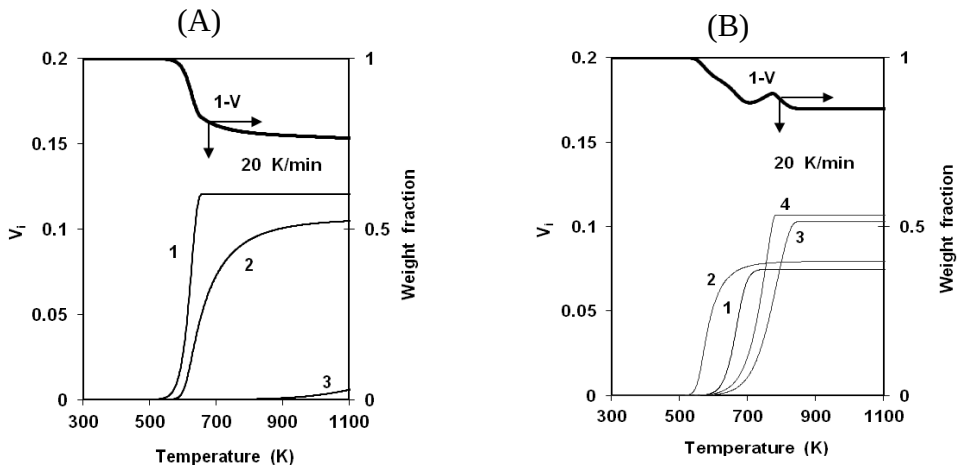

Figure 6. Pyrolysis runs of the non metallic sample: (A) Dynamic experimental runs at three heating rates (the calculated curves overlap the experimental ones) and DTA curve for the run at 20 K min^{-1}. (B) TG and DTG curves (experimental and calculated) at 20 K min^{-1}. (C) Isothermal TG curves (experimental and calculated) at different heating rates.

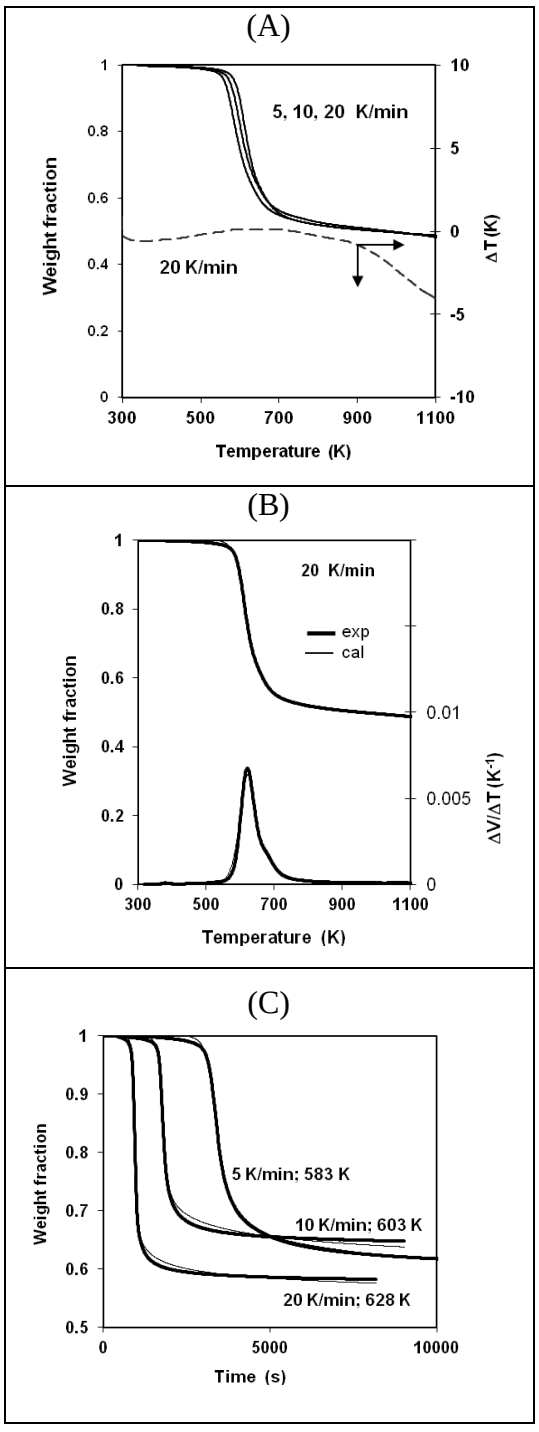

Figure 7. Different combustion runs of non metallic printed circuit boards in N_2:O_2 = 4:1 atmosphere (experimental and calculated curves): (A) Dynamic TG curves at 5, 10 and 20 K min^{-1} and DTA curve for the run at 20 K min^{-1}. (B) TG and DTG run at 20 K min^{-1}. (C) TG isothermal curves at different heating rates.

Poner curvas experimentales en (A)

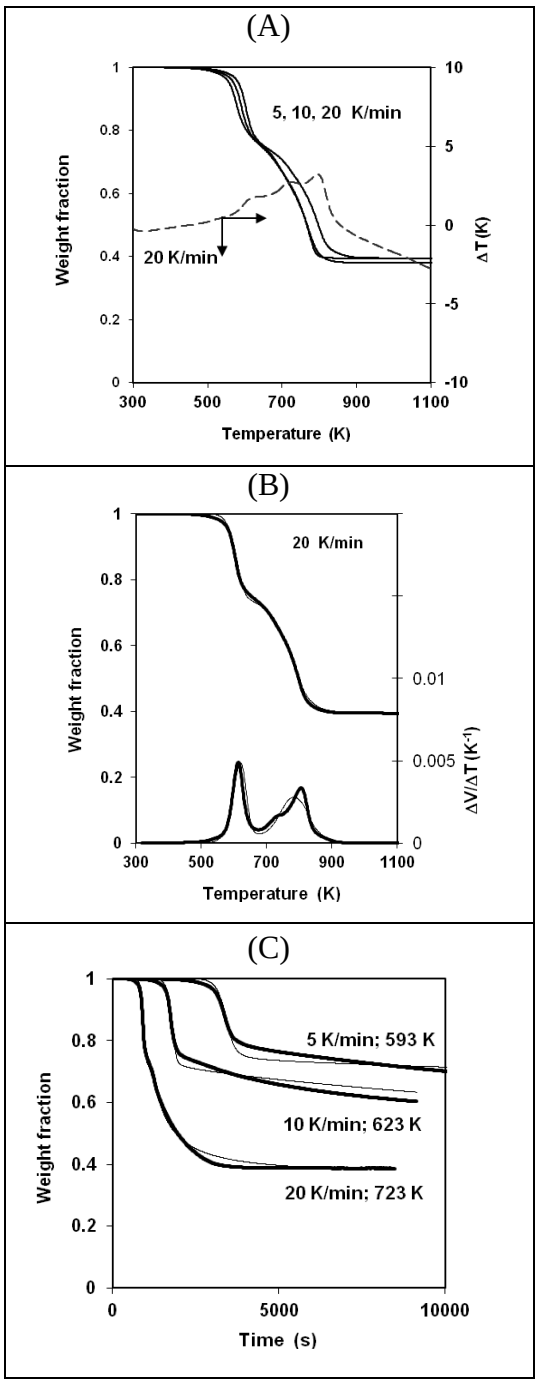

Figure 8. Different combustion runs of non metallic PCB in N_2:O_2 = 9:1 atmosphere at 5, 10 and 20 K min^{-1} (experimental and calculated curves): (A) Dynamic TG runs. (B) Isothermal TG runs.

Poner curvas experimentales en (A)

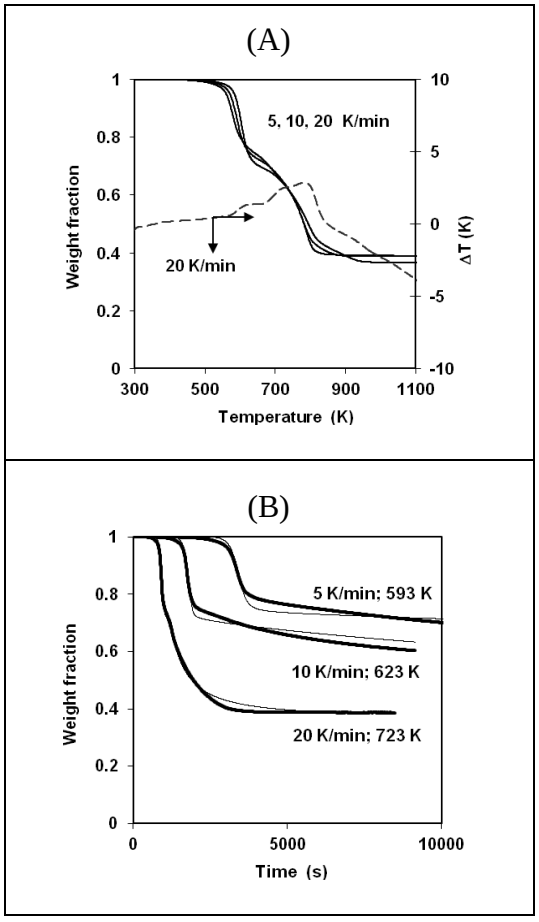

619 Figure 9. TG-MS of non metallic printed circuit boards at a heating rate of 30 K min^{-1}:
620 (A) Intensity of ions m/z 18 (water), 28 (CO) and 44 (CO_2) in pyrolysis (He). (B)
621 Intensity of ions m/z 16 (methane), 27 (ethylene), 41 (propylene) and 94 (phenol) in
622 pyrolysis (He). (C) and (D) Intensity of the same ions as (A) and (B) in combustion
623 (He:O_2 4:1).

624

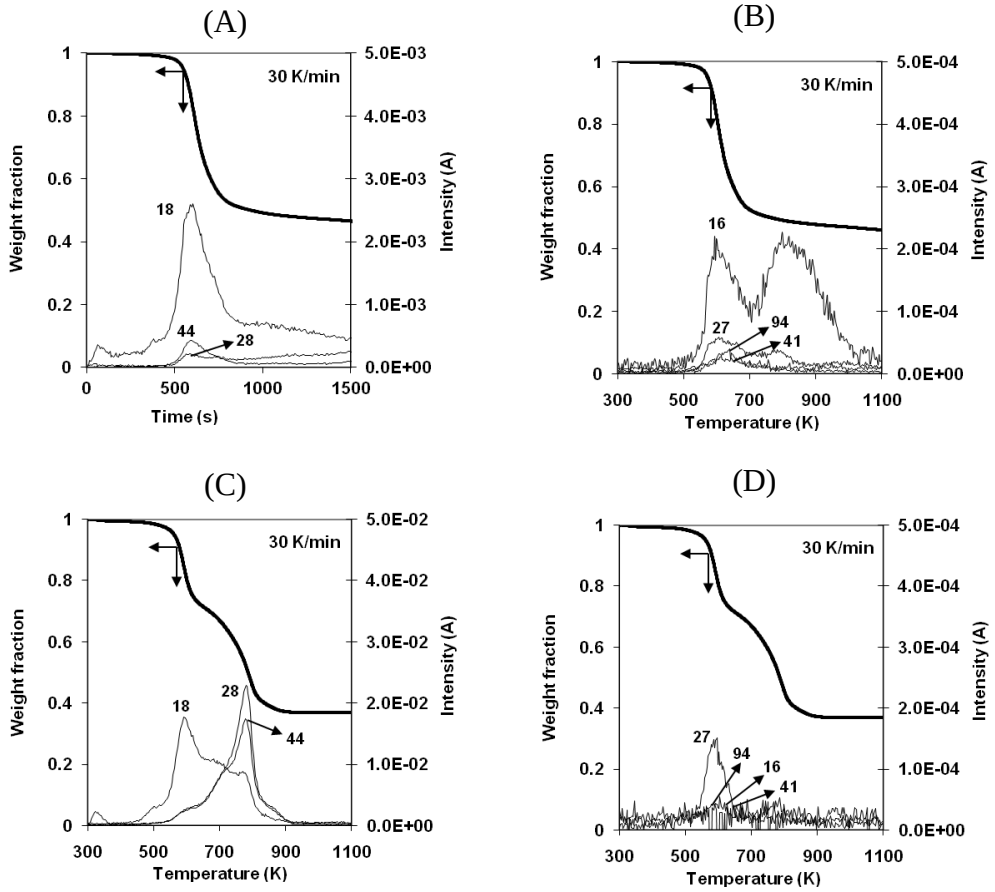

625

626

627 Figure 10. Evolution of the weight mass and the weight fraction of residues for each
628 reaction, non metallic PCB sample: (A) Pyrolysis TG run. (B) Combustion TG run
629 (N_2:O_2 = 4:1 atmosphere).

630 CAMBIAR TAMBIÉN PARA QUE BAJEN LOS VOLÁTILES?

631

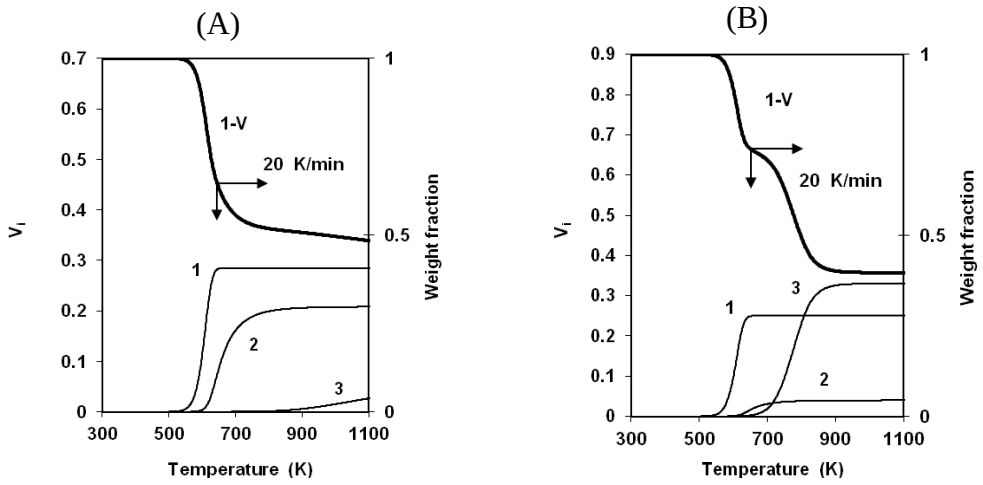

632